J. Phase Equilib. Diffus. (2023) 44:429–444
https://doi.org/10.1007/s11669-023-01049-9

ORIGINAL RESEARCH ARTICLE

Different Approach to Thermodynamic Description of Bi-Te Binary System

S. Drzewowska[1] · **B. Onderka**[1]

Submitted: 29 March 2023 / in revised form: 2 May 2023 / Accepted: 29 May 2023 / Published online: 4 July 2023

Abstract The aim this work was the reinvestigation of phase equilibria in Bi-Te system. The as-cast and long-time equilibrated alloys of Bi-Te binary system were analysed by scanning electron microscopy, X-ray diffraction (XRD) and differential thermal analysis (DTA) methods. The primary solidified phases were identified for as-cast samples. The existence of the four intermetallic phases: Bi_2Te_3, BiTe, Bi_2Te, Bi_7Te_3 was confirmed. Three of them melt incongruently in peritectic reactions. The model parameters of all phases in this system were assessed by optimization using available data by Calphad method. The stabilisation of these phases in other ternary systems was discussed taking into consideration its future application in thermodynamic description of Ag-Bi-Te ternary system.

Keywords Bi-Te · binary alloys · calphad · phase diagram · thermodynamics

1 Introduction

The Peltier effect in a thermocouple incorporating bismuth telluride, Bi_2Te_3 was observed more than 60 years ago.[1] From that time this compound has been extensively used in the construction of different thermoelectric modules.[2] The performance of these modules depends on the number of factors which are combined in the thermoelectric figure of merit, ZT, where Z is defined as $\alpha^2\sigma/\lambda$, (α is the Seebeck coefficient, σ is the electrical conductivity and λ is the thermal conductivity). Optimizing ZT is a nontrivial task because the variables in ZT, despite of separate expression are in fact coupled to each other. From the beginning the optimization of the charge carrier concentration and reduction of the lattice component of the thermal conductivity, λ_L were achieved through the use of solid solutions of bismuth telluride with the isomorphous compounds antimony telluride and bismuth selenide.[3] The enhanced scattering of phonons in these solid solutions is not usually accompanied by a reduction in the mobility of the charge carriers. It has been found that Bi_2Te_3-based alloys have the relatively highest ZT near room temperature ($\sim$300 K). Such alloys used in solid-state devices dominate the market for temperature control in optoelectronics. Peltier cooling is also more and more attractive particularly in small systems to eliminate greenhouse-gas refrigerants. Since thermoelectric technology will be greatly enhanced by improving Bi_2Te_3, numerous attempts have been made to discover better materials which requires the knowledge of the stability of phases in Bi-Te system.

At the beginning the inconsistency in Bi-Te phase diagram was observed, especially in solid-liquid equilibria in the Bi-rich part of the system. To explain such a discrepancy in experimental data Brebrick[4] concluded that a continuous sequence of ordered phases formed as Bi_mTe_n, can be interpreted as solid solutions without arbitrary choice of m and n. He also suggested[4] that the bismuth layers of Bi_4Te_5 may arise from antistructure defects of tellurium atoms which must lead to a homogeneity region in the compounds. Brebrick[4] also suggested the existence of two different versions of phase diagrams for the Bi-Te system. The first metastable phase diagram, corresponding to differential thermal analysis (DTA) and solid state

✉ B. Onderka
onderka@agh.edu.pl

[1] Department of Non-Ferrous Metals, AGH University of Science and Technology, 30 Mickiewicza Ave., 30-059 Kraków, Poland

synthesis conditions with extensive regions of solid solution. The equilibrated second one, requires the synthesis of intermetallic compounds. Next, Anderson[5] proposed to describe the crystal structure of solid phases in Bi-Te system as the structures built by the ordered repetition of a common hexagonal sub-cell along c-axis with a minimum adjustment of atomic positions with composition. Such a repetition of a set of sub-cells differs in compositions but are structurally closely related. The stoichiometry of compounds obtained from such repetition can be additionally affected by probable replacement of Bi by Te at a level of 1 at.%. Consequently, Bos et al.[6] examining the series of alloys in range from Bi to Bi_2Te_3 derived the crystal structures as an ordered stacking of Bi_2Te_3 and Bi_2 building blocks. All phases in the bismuth tellurides together with terminal solution of (Bi) can be recognized as homologous series of $(Bi_2)_m(Bi_2Te_3)_n$ type: Bi_2Te_3 (m:n = 0:3), Bi_4Te_5 (m:n = 1:5), Bi_6Te_7 (m:n = 2:7), Bi_8Te_9 (m:n = 9:3), BiTe (m:n = 1:2), Bi_4Te_3 (m:n = 3:3), Bi_2Te (m:n = 2:1), Bi_7Te_3 (m:n = 15:6), and Bi (m:n = 3:0). The existence of $Bi_{10}Te_9$ (m:n = 6:9) has been additionally predicted.[7, 8]

In order to analyse the experimentally obtained liquidus projection and isothermal section at the 523 K of the Bi-In-Te ternary system Chen and co-workers[9] proposed the simplification of the Bi-Te system by grouping the undetermined binary phases between Bi and Bi_2Te_3 as a $(Bi_2)_m(Bi_2Te_3)_n$ phase.

The p-T-x literature data of Bi-Te phase system up to the year 1994, with special attention to Russian publications, had been reviewed by Chizevskaya et al.[10] and the T-x diagram was assessed. The characteristics of Bi_2Te_3 solid- liquid and solid-gas transitions were analysed. Additionally, the crystal data of existing detected phases were summarized together with thermodynamic functions. Chizevskaya et al.[10] using cubic spline analysis[11] combined with thermodynamic rules critically assessed the parts of liquidus line starting from crystallization points of solid compounds.

Based on the DSC results and morphology difference of scanning electron microscopy/back scattered electron (SEM/BSE) images of samples annealed in different temperatures Mao et al.[12] put forward the Bi-Te phase diagram. They assumed that the single solid solution denoted as β phase represents the superstructure of the $(Bi_2)_n(Bi_2Te_3)_m$ homologous series. Additionally, Mao et al.[12] had taken into consideration compounds Bi_4Te_3 and Bi_2Te modelled as the intermetallic compounds, i.e. line compounds. But the proposed thermal stability ranges of Bi_2Te and Bi_4Te_3 compounds are very narrow, 30 and 20 K, respectively. It should be emphasised that such stability ranges are rather unusual.

In 2008 the thermodynamics and topology of bismuth-tellurium system were critically reviewed by Mao et al.[12] and Gierlotka.[13] They both emphasized that the phase diagram of Bi-Te system had several versions that did not agree. The observed inconsistency of the phase equilibria concentrates in Bi-Bi_2Te_3 part of compositions in which a layered structure of solid phases was determined.

Coupling their experimental results with the literature thermodynamic and topological data Mao et al.[12] assessed the Bi-Te binary system using Calphad (calculation of phase diagrams) technique. In their approach, the β phase was described by the two sublattice $(Bi)_2(Bi,Te)_3$ model. It seems that the stoichiometric ratio of β phase can be recognized as phase BiTe which composition deviating from stoichiometric ratio to higher Bi content as the temperature decreases.

All other telluride phases Mao et al.[12] modeled as the stoichiometric compounds and the liquid solution as a substitutional solution. The lack of detectable mutual solubility in terminal solutions of Bi and Te was neglected in phase modelling.

Considering Mao's[12] work, Gierlotka[13] took into consideration the thermodynamic data of Bi_2Te_3 phase determined at 298 K by Howlett et al.[14], Boncheva-Mladenova et al.[15], Vecher et al.[16], Wagman et al.[17] and Sidorko et al.[18] In his reassessment of Bi-Te system[13] the possible clustering in liquid phase[19–22] was taken into account, and consequently the liquid solution was modelled as the associate liquid solution.[23] According to Brebrick results[24] the narrow homogeneity range (59.7 and 60.2 Te at.%) of Bi_2Te_3 compound was described by Wagner-Schottky model.[25]

In 2015 Kifune et al.[26] found that the boundary of the compound homologous series is Bi_8Te_3 (27.3 at.% Te) single phase instead of the Bi_7Te_3 (30.0 at.% Te) phase in the Bi-rich boundary.[6, 27] Using Rietveld method, the homologous phase is a four-dimensional superstructure of space group $R\bar{3}m$. This experimental data do not correspond to the data presented by Mao et al.[12] and in Gierlotka's[13] assessments as well.

In turn, Babanly et al.[28] observed the existence of stable $Bi_{14}Te_6$ compound and Bi_2Te, BiTe, and Bi_2Te_3 compounds with restricted range of homogeneity (non-stoichiometric). The boundaries between the intermediate phases in the Bi-Te system were determined via electromotive force (EMF) method[28] and agree with the data derived from physicochemical analysis.[29] It seems that these results confirm stability of Bi_2Te and BiTe phases in the low temperature range. The existence of the compounds Bi_2Te_3, BiTe, Bi_2Te and $Bi_{14}Te_6$ was also confirmed in the study of Bi-Te-I system by Babanly's group.[30] Very similar result was obtained by Prokhorenko et al.[31] in the range of

495–550 K using thermal titration method.[32, 33] Prokhorenko et al.[31] noticed that intermediate variable-composition Bi_2Te_3, BiTe, Bi_2Te, and $Bi_{14}Te_6$ phases form in the partial ternary Bi-Ag_2Te-Bi_2Te_3 system. The triangulation of the ternary Ag_2Te-Bi-Bi_2Te_3 system within a temperature range of 300–600 K agrees well with the literature data of Babanly et al.[28, 30]

The conclusions of experimental work from Babanly et al.[28, 30] and Prokhorenko et al.[31] also do not agree with data presented by Mao et al.[12] According to these results[28] it seems that the addition of third element to bismuth tellurides can stabilize them as solid compounds. To obtain the thermodynamic description of Ag-Bi-Te and Bi-Te-I systems agreeing with their results, it is necessary to assess the Bi-Te phase diagram with binary phases where the stability was confirmed in ternaries.[28, 30, 31] Taking into account the results of the analysis of Ag-Bi-Te system[28, 31] the stabilisation of binary tellurides can be expected with Ag addition in ternary Ag-Bi-Te alloys.

Consequently, the aim of the present work is the analysis of phase equilibria in Bi-Te system and optimization of model parameters of phases in this system to be next applied in Ag-Bi-Te ternary system description by Calphad method. The compositions of the six Bi-Te alloys were selected to enable the identification of the phases: Bi_2Te_3, BiTe, Bi_2Te, Bi_7Te_3. The phase BiTe corresponds to the β phase in the assessments of Mao et al.[12] and Gierlotka.[13] The $Bi_{14}Te_6$ phase corresponds to the stoichiometry of the Bi_7Te_3 phase which was described by Glazov et al.[20] and by Chizhevskaya et al.[10] The annealing temperatures were selected below the liquidus temperature for the Bi-Te two-component system based on the work of Chizhevskaya et al.[10]

2 Materials and Experimental Methods

The Bi-Te alloys were prepared from high purity metals: Bi 99.997 wt.% (Alfa Aesar, USA) and Te 99.9999 wt.% (Alfa Aesar, USA). The theoretical composition of alloy samples (no. 1–6) are given in Table 1. The weighed amounts of pure metals (~2 g) were sealed in quartz tube under vacuum and then fused and molten in furnace at 700 °C for 24 h to mix together, followed by water quenching. Additionally, intermetallic phase Bi_2Te of stoichiometric composition was prepared by the same procedure as above, with different melting temperature–600 °C.

Due to the relatively high evaporation rates of bismuth and tellurium,[21, 24, 34–36] to avoid a significant change in the chemical composition of the alloys samples during the sealing process in quartz ampoules, each of the elements was added with a slight excess: ~ 80 mg, and ~ 60 mg for bismuth and tellurium, respectively.

Next, the samples were weighed again to control the possible mass loss during the sample preparation according to the relatively high tellurium partial pressure at operation temperatures.[12, 37] After synthesis the samples were isothermally equilibrated at the chosen temperatures according to the following procedure: The as-cast weighed Bi-Te alloy samples (~1 g) were sealed in quartz tubes under vacuum again and then annealed below the solidus. The appropriate temperatures were applied for individual alloys to achieve equilibrium (Table 1). It is well known that the bulk samples of layered Bi-Te phases obtained by melting of pure components do not reach an equilibrium state even after a long period 84–125 days of thermal annealing.[27, 29, 37] Due to very low diffusion rates between layers the non-equilibrium phase constitution obtained by cooling from liquid solution only changes slightly during further heat treatment. Based on older literature data (details in the discussion) and the latest experimental investigations of Mao et al.[12] it was decided in the current work to equilibrate Bi-Te alloys isothermally for 30 and 60 days at appropriate temperatures. After long-term annealing, the samples were quenched into iced water to maintain high-temperature phase composition. The annealed samples were cut into parts for the different examinations.

The obtained microstructure was observed by scanning electron microscopy (SEM) (Hitachi, SU-70, Japan, with electron microprobe ThermoScientific, with ZAF correction). For qualitative and quantitative analysis, the EDX (Energy Dispersive X-ray Spectroscopy) method was

Table 1 Constitution of Bi-Te alloys and heat treatment parameters, as a process temperature and an annealing time for equilibrated alloys

Sample no.	Sample composition, at.%		Mass loss of as-cast alloy in %	Temperature, °C	Annealing time, days
	Bi	Te			
1	30	70	0.42	390	60
2	40	60	0.78	480	30
3	45	55	0.11	480	30
4	60	40	1.15	390	60
5	68	32	0.10	240	60
6	80	20	0.45	240	60

applied. Four samples (Bi60Te40, Bi68Te32, Bi80Te20 and the Bi_2Te phase sample) were additionally analysed using FEI Quanta 3D FEG-SEM scanning electron microscope with an EDAX APOLLO energy dispersion x-ray spectrometer. The phase constitution of studied alloys was determined by x-ray Powder Diffraction (XRD) method using Rigaku Japan MiniFlex II x-ray Diffractometer with Cu-Kα radiation.

DTA measurements were performed with the use of DSC/DTA Pegasus 404 F1 (Netzsch, Germany) scanning calorimeter with a DTA probe. The samples were sealed in evacuated silica tubes and placed at the DTA sensor in a platinum crucible. An empty evacuated silica tube of similar mass was used in a second platinum crucible as a reference. No traces of Te evaporation were observed at inner surface of quartz tubes after measurements. The thermal analysis was carried out in cycles with heating rates of 2 as well as 5 and 10 deg/min (for specified sample compositions). The compositions of all alloys in atomic percent used in our studies are presented in the Table 1.

3 Results

Table 1 summarizes chemical composition, weight loss during casting, and the isothermal equilibration parameters: temperature and an annealing time of the alloys for the Bi-Te two-component system. After melting process, the mass loss was generally below 1% (Table 1), this was not only due to Te evaporation but also to partial sticking of samples to the glass surface of the silica tube (above 1% mass loss of sample 4). So, after synthesis the composition of Bi-Te alloys remained unchanged in the experimental error range. Also, no significant evaporation of sample components was observed during isothermal annealing.

Tables 2 and 3 present the XRD, EDX results for as-cast and annealed Bi-Te alloys (Table 1). Bi_2Te_3 as the primary phase was observed for alloys samples: Bi30Te70, Bi40Te60, Bi45Te55, on the back-scattered electron image (BEI) micrograph, while BiTe as primary phase was determined for alloys Bi60Te40, Bi68Te32, Bi80Te20 (Fig. 2).

Annealed alloys samples with the following compositions: Bi60Te40, Bi68Te32, Bi80Te20 and the Bi_2Te phase sample (Table 3) were also analysed on the SEM FEI Quanta 3D FEG-SEM microscope. The detected primary phases in the listed alloys are consistent for both series of measurements.

The DTA results of alloys no. 1-6 and phase Bi_2Te are shown in Table 4 for three different heating rates: 2, 5, 10 deg/min. Some data of the second heating cycle was also shown. From the cooling cycle data at different rates significant undercooling of liquid samples was determined. As an example, the onset data of liquidus points of different samples cooled with the different rates are shown in Table 4. DTA results for 2 deg/min first heating cycle are shown in Fig. 1.

Figure 2 and 3 show BEI micrographs of as-cast and annealed Bi-Te alloys. Detected phases are identified in the images. BEI micrograph of as-cast (non-equilibrated) alloy Bi30Te70 (no. 1) of the composition 70 at.% Te is shown in Fig. 2(a). The microstructure consists of: light elongated lamellar grains of Bi_2Te_3 phase, dark narrow areas around the Bi_2Te_3 plates which are tellurium phase, and needle-shaped solidified liquid phase of eutectic composition. The composition of the brightest phase Bi_2Te_3 was measured to be 66.29 at.% Te and that of the dark narrow areas of (Te) phase is 98.76 at.% Te.

Figure 2(b) is BEI micrograph of as-cast alloy no. 2 with the atomic composition of Bi40Te60. The structure is composed of mixed eutectic grains and the remainder are elongated grains of the Bi_2Te_3 phase with different shades of grey resulting from different orientations. The composition of the grey grains of Bi_2Te_3 phase is 61.78 at.% Te.

In Figure 2(c–g) the BEI micrographs of as-cast alloys no. 3-7 with the compositions: Bi45Te55, Bi60Te40, Bi68Te32, Bi80Te20, Bi67Te33 are shown. All these alloys have three distinct areas. The bright matrix is (Bi) phase (Fig. 2c–g). The amount of Te in the phase (Bi) was determined as 3.68 and 0.78 at.% Te for Bi45Te55 and Bi60Te40 samples, respectively. For the other alloys (Bi68Te32, Bi80Te20, Bi67Te33) no trace of Te was observed in (Bi) phase.

Figure 2(c) shows dark elongated grains of Bi_2Te_3 phase with the composition 59.32 at.% Te and grey precipitates of BiTe phase with composition 44.26 at.% Te. In Fig. 2(d), (e), (g) the darkest elongated lamellar grains are the BiTe phase, and the grey interphase regions are the Bi_2Te phase. The compositions of BiTe are 49.02, 45.80 and 40.94 at.% Te, and of Bi_2Te are 38.14, 34.53, 34.07 at.% Te for samples no. 4, 5 and Bi_2Te phase, respectively. The different shades of grey observed for Bi_2Te sample correspond to different crystal orientations of the grains. The situation is similar for the Bi_2Te_3 phase in Figure 3(b) for the equilibrated alloy with the composition Bi40Te60. The microstructure of as-cast Bi80Te20 (no. 6) alloy consists of the bright (Bi) phase, the dark lamellar grains of BiTe phase and the grey precipitates of Bi_7Te_3 phase (Fig. 2f). The composition of tellurium for BiTe, and Bi_7Te_3 phases was determined as 43.93 and 30.23 at.%, respectively. The primary solidified phases identified from microstructures (Fig. 2(a–g) are shown in last column in Table 2.

The BEI micrograph of annealed alloy of composition Bi30Te70 (no. 1) equilibrated at 390 °C during 60 days is shown in Figure 3(a). Its two-phase microstructure is

Table 2 Experimental results (XRD, EDX data) for as-cast alloy samples

Sample composition, at.%	XRD results		EDX results, at.%			Primary solidification phase
	Phase	Chart no.	Bi	Te	Phases	
Bi30Te70	Bi_2Te_3	01-076-2813	33.71	66.29	Bi_2Te_3	Bi_2Te_3
	(Te)	01-085-0554	1.24	98.76	(Te)	
			17.17	82.83	eutectic	
Bi40Te60	Bi_2Te_3	01-076-2813	37.22	62.78	Bi_2Te_3	Bi_2Te_3
			24.72	75.28	eutectic	
Bi45Te55	Bi_2Te_3	01-076-2813	40.68	59.32	Bi_2Te_3	Bi_2Te_3
	BiTe	01-075-1095	55.74	44.26	BiTe	
	(Bi)	01-085-1330	96.33	3.68	(Bi)	
Bi60Te40	BiTe	01-075-1095	50.99	49.02	BiTe	BiTe
	(Bi)	01-085-1330	99.22	0.78	(Bi)	
	Bi_2Te	00-042-0540	61.86	38.14	Bi_2Te	
Bi68Te32	Bi_2Te	00-042-0540	65.48	34.53	Bi_2Te	BiTe
	BiTe	01-075-1095	54.20	45.80	BiTe	
	(Bi)	01-085-1329	100	0.00	(Bi)	
Bi80Te20	Bi_7Te_3	00-012-0719	69.77	30.23	Bi_7Te_3	BiTe
	BiTe	01-083-1749	56.07	43.93	BiTe	
	(Bi)	01-085-1329	100	0.00	(Bi)	
Bi_2Te	Bi_2Te	00-042-0540	65.93	34.07	Bi_2Te	Bi_2Te
	BiTe	01-083-1749	59.06	40.94	BiTe	
	(Bi)	01-085-1329	100	0	(Bi)	

Table 3 Experimental results (XRD, EDX data) for annealed alloy samples

Sample composition, at.%	XRD results		EDX results, at.%		
	Phases	Chart no.	Bi	Te	Phases
Bi30Te70	Bi_2Te_3	01-076-2813	38.27	61.73	Bi_2Te_3
	(Te)	01-085-0554	0	100	(Te)
Bi40Te60	Bi_2Te_3	01-085-0439	38.58	61.42	Bi_2Te_3
Bi45Te55	BiTe	01-075-1095	42.57	57.43	BiTe
Bi60Te40	BiTe	01-083-1749	55.90	44.10	BiTe
	Bi_2Te	00-042-0540	66.45	33.55	Bi_2Te
	(Bi)	00-044-1246	100	0	(Bi)
Bi68Te32	Bi_2Te	00-042-0540	65.89	34.11	Bi_2Te
Bi80Te20	Bi_7Te_3	00-012-0719	69.95	30.05	Bi_7Te_3
	(Bi)	00-044-1246	100	0	(Bi)

composed of large light lamellar grains of the Bi_2Te_3 phase with average chemical composition of 38.3 at.% Bi (61.7 at.% Te). The image does not show the fine eutectic as in as-cast alloy but a mixture of dark areas of almost pure tellurium (Te) ($\sim$100 at.% Te) phase with the light grains of Bi_2Te_3 compound can be observed. In Figure 3(b) the BEI micrograph of alloy no. 2 with the composition of Bi40Te60 equilibrated at 480 °C for 30 days is shown. The microstructure is single phase with Bi_2Te_3 phase of composition 38.6 at.% Bi (61.4 at.% Te) with different shades of grey resulting from different grain orientations.

In Figure 3(c) the BEI micrograph of annealed alloy no. 3 (composition of Bi45Te55) equilibrated over 30 days at 480 °C is shown. Its microstructure consists of single-phase lamellar grains arranged in different orientations which are the BiTe phase with chemical composition 42.6 at.% Bi (57.4 at.% Te). They also have different shades of grey. The phases (Bi) and Bi_2Te_3 observed in as-cast alloy sample disappeared after annealing.

Table 4 DTA results for annealed samples and Bi_2Te as-cast phase for cycles of different heating rates: 2, 5 and 10 deg/min

No. Sample	Composition, at.% Te	Heating rate, deg/min	Temperature of heat effect, °C	Heating rate, deg/min	Temperature of heat effect, °C	Heating rate, deg/min	Temperature of heat effect, °C
1	70	2	417.0		…	10	416.8
			564.5		…		571.8
			416.5*		…		415.8*
			564.7*		…		577.3*
			538.9↓		…		536.3↓
			400.7↓		…		396.0↓
2	60	2	586.2		…	10	585.5
			586.8*		…		586.1*
			568.9↓		…		578.0↓
3	55	2	537.2	5	556.9	10	377.3
			556.3		586.1		554.9
			561.9		557.6*		588.8
			583.6		563.5*		548.5*
			556.7*		586.2*		585.3*
			562.5*		563.7↓		573.8↓
			584.1*		548.2↓		543.4↓
			571.3↓		…		…
			552.9↓		…		…
4	40	2	265.4	5	266.0	10	262.5
			427.0		426.8		424.5
			521.7		520.4		524.0
			266.2*		265.9*		263.8*
			426.5*		426.8*		423.8*
			520.3*		520.3*		523.1*
			513.4↓		507.4↓		507.3↓
			415.5↓		398.5↓		255.6↓
			262.9↓		260.2↓		…
5	32	2	265.4	5	266.4	10	314.1
			307.9		309.6		427.0
			426.9		425.3		474.4
			484.9		485.4		264.5*
			266.2*		266.1*		423.7*
			425.4*		425.0*		478.0*
			483.2*		485.0*		464.6↓
			474.9↓		472.6↓		254.7↓
			263.1↓		260.3↓		
6	20	2	266.3	5	266.9	10	266.9
			309.0		423.9		319.1
			427.0		266.2*		414.3
			266.4*		422.7*		265.6*
			419.7*		415.7↓		418.3*
			418.5↓		250.9↓		411.8↓
			262.9↓		…		254.4↓
7	33.3		…		…	10	264.2
			…		…		428.5
			…		…		487.0
			…		…		264.8*

Table 4 continued

No. Sample	Composition, at.% Te	Heating rate, deg/min	Temperature of heat effect, °C	Heating rate, deg/min	Temperature of heat effect, °C	Heating rate, deg/min	Temperature of heat effect, °C
			…		…		486.0*
			…		…		476.9↓
			…		…		255.1↓

* – second heating cycle, ↓ – cooling cycle

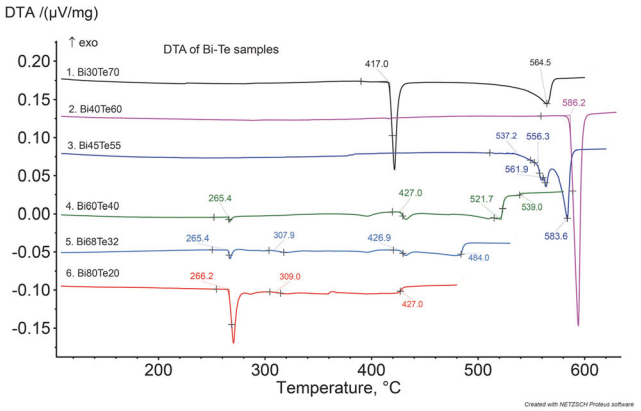

Fig. 1 DTA results for 2 deg/min heating rate. The first heating cycle was shown

The next BEI micrograph shows the microstructure of alloy no. 4 (Bi60Te40) after 60 days of equilibration at 390 °C (Fig. 3d). It consists of three-phases: the bright pure bismuth phase (Bi) (~100 at.% Bi), lamellar grains with different shades of grey, which are the BiTe phase with average chemical composition 55.9 at.% Bi (44.1 at.% Te), and the Bi_2Te phase which forms lighter precipitates at grain boundaries (33.5 at.% Te). The grains of BiTe phase are much larger than in as-cast microstructure and the (Bi) phase is still present. So, it seems that in this sample the equilibration was not finished during annealing process. The presence of (Bi) phase in samples annealed at low temperature and did not reach equilibrium was described in literature.

In Figure 3(e) the BEI micrograph of alloy Bi68Te32 (no. 5) equilibrated at 240 °C over 60 days is presented. It is evident that this no longer a 3-phase microstructure as the as-cast alloy. Instead, it is the single-phase structure of Bi_2Te with the average chemical composition of 65.9 at.% Bi (34.1 at.% Te). The micrograph of alloy Bi80Te20 (no. 6) annealed at 240 °C over 60 days is shown in Figure 3(f). The two-phase microstructure is composed of the bright bismuth (Bi) phase (~100 at.% Bi) and a dark-grey areas assigned to Bi_7Te_3 phase with Bi content of 70 at.% (30 at.% Te), which is the microstructure of a ripened hypereutectic.

Figure 4 presents compiled normalized XRD diffractograms of annealed alloys no. 1-6. The number of phases in diffractograms for Bi30Te70, Bi40Te60, Bi45Te55, Bi68Te32, Bi80Te20 annealed alloys coincides with number of phases in micrographs from SEM analysis and EDX results. Diffractogram of Bi60Te40 alloy indicates two phases: BiTe and Bi_2Te.

3.1 The Assessment of Bi-Te Phase System

As was mentioned previously, taking into accountg data obtained in present work the following phases are considered in this work: liquid, rhombohedral_A7 (Bi), hexagonal_A8 (Te), Bi_2Te_3, β(BiTe), Bi_2Te, and Bi_7Te_3 ($Bi_{14}Te_6$).

The Gibbs free energies of pure elements $G_i^0(T) = G_i(T) - H_i^{SER}(298)$ are the following functions of temperature (Eq 2):

$$G_i^0(T) = a + bT + cT\ln T + dT^2 + eT^{-1} + fT^3 + iT^4 + jT^7 + kT^{-9} \quad \text{(Eq 1)}$$

The $G_i^0(T)$ functions are referred to the enthalpy values $H_i^{SER}(298)$ of the standard element reference *SER* at 298.15 K and 1 bar as recommended by SGTE Group[1].[38] The reference states are pure elements Bi and Te with rhombohedral_A7 and hexagonal_A8 structure, respectively. The expression Eq 2 may be used for several temperature ranges, with different set of coefficients (*a, b, c, d, e, f, i, j, k*) in each. The $G_i^0(T)$ functions are taken from thermodynamic database SGTE Unary TDB v.5[38] for pure elements.

3.2 Rhombohedral_A7 (Bi) and Hexagonal_A8 (Te) Terminal Phases

Experimental information does not indicate mutual solubility of Bi and Te. So, both phases were described as pure elements and their Gibbs energies were taken from the unary elements database.[38]

[1] Scientific Group Thermodata Europe.

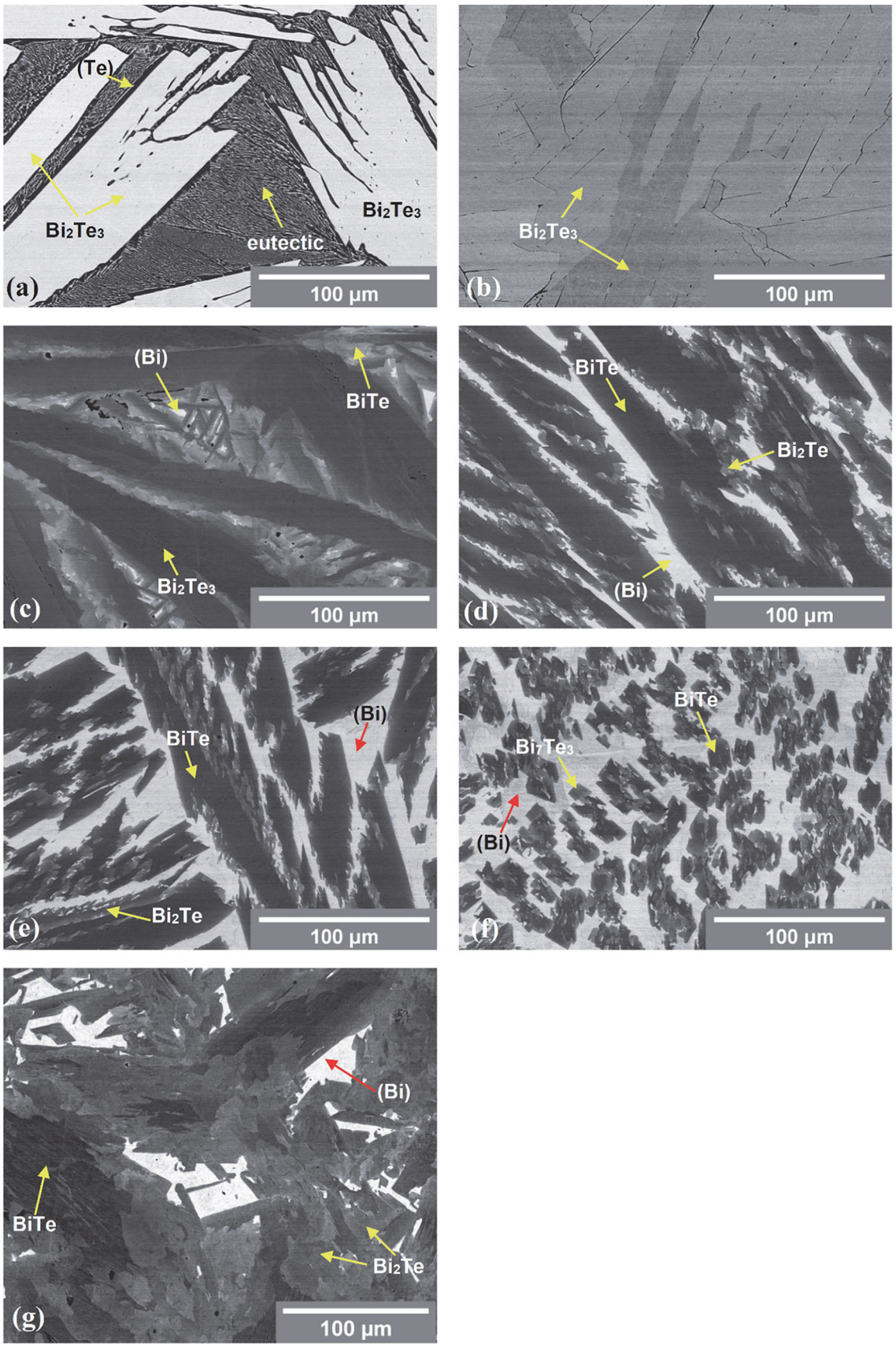
(Te)
Bi2Te3
Bi2Te3
eutectic
(a)
100 μm
Bi2Te3
(b)
100 μm
(Bi)
BiTe
Bi2Te3
(c)
100 μm
BiTe
Bi2Te
(Bi)
(d)
100 μm
BiTe
(Bi)
Bi2Te
(e)
100 μm
BiTe
Bi7Te3
(Bi)
(f)
100 μm
(Bi)
BiTe
Bi2Te
(g)
100 μm

◀**Fig. 2** Back-scattered electron image micrographs of Bi-Te as-cast alloys: (a) Bi30Te70 alloy showing Bi_2Te_3+eutectic+(Te) microstructure; (b) Bi40Te60 alloy showing Bi_2Te_3+eutectic microstructure; (c) Bi45Te55 alloy showing BiTe+Bi_2Te_3+(Bi) three-phase microstructure; (d) Bi60Te40 alloy showing BiTe+Bi_2Te+(Bi) three-phase microstructure; (e) Bi68Te32 alloy showing BiTe+Bi_2Te+(Bi) three-phase microstructure; (f) Bi80Te20 alloy showing BiTe+Bi_7Te_3+(Bi) three-phase microstructure; (g) phase Bi_2Te with Bi67Te33 composition showing BiTe+Bi_2Te+(Bi) three-phase microstructure (image of FEI Quanta 3D FEG-SEM electron microscope)

3.3 Bi_7Te_3 and Bi_2Te Phases

These phases are modelled as the line compounds. Their heat capacity has not been determined yet, therefore their Gibbs energy is described according to the Neumann-Kopp rule:

$$G^{Bi_mTe_n}_{Bi:Te} = A + BT + m \cdot^0 G^{\text{rom}}_{Bi} + n \cdot^0 G^{\text{hex}}_{Te} \quad \text{(Eq 2)}$$

where T is an absolute temperature, A and B are adjustable parameters. Numbers m and n are the

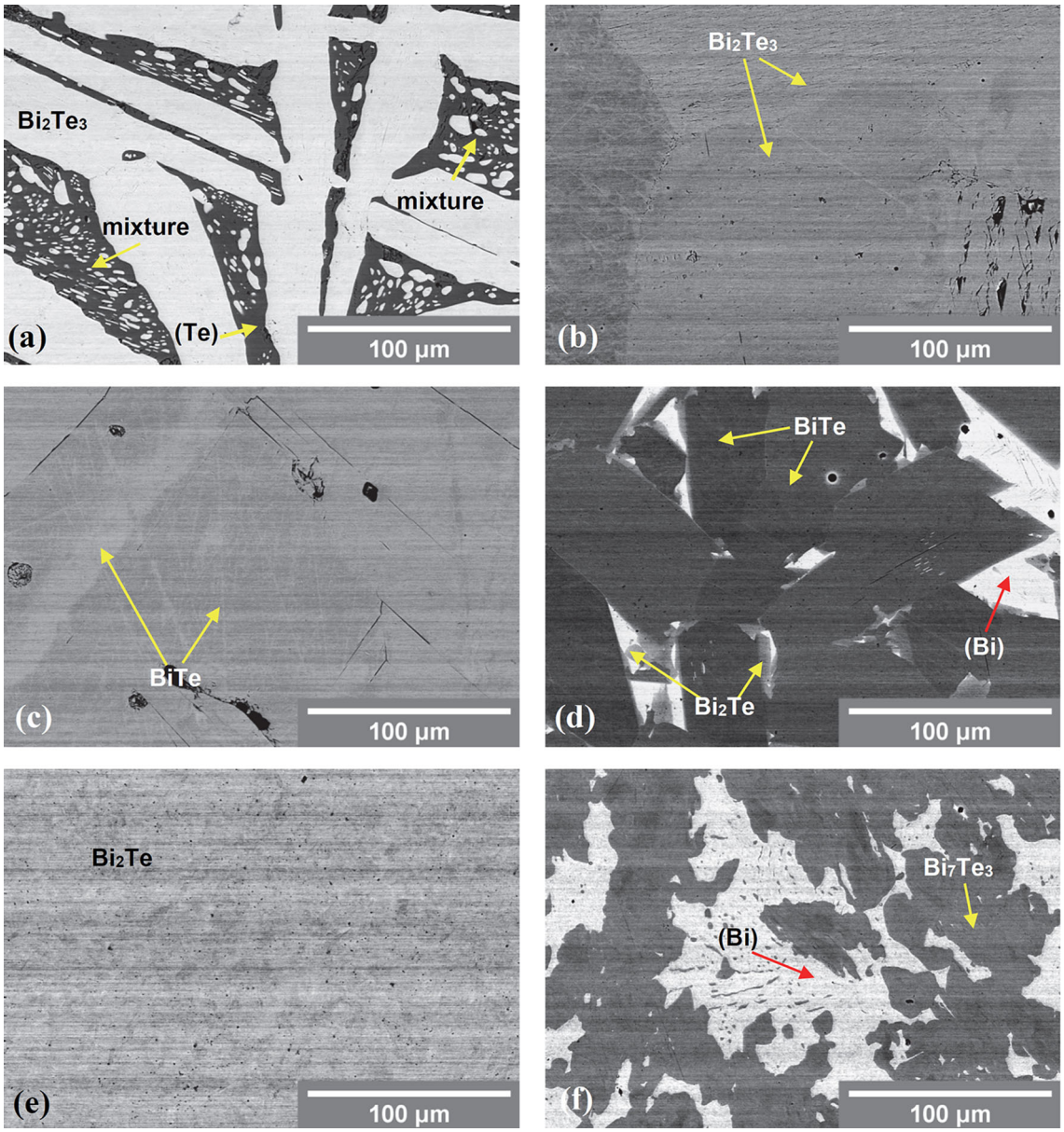

Fig. 3 BEI micrographs of Bi-Te of annealed alloys: (a) Bi30Te70 alloy showing Bi_2Te_3 + Te+post-eutectic mixture microstructure; (b) Bi40Te60 alloy of Bi_2Te_3 one-phase microstructure; (c) Bi45Te55 alloy of BiTe one-phase microstructure; (d) Bi60Te40 alloy showing BiTe+Bi_2Te two-phase microstructure; (e) Bi68Te32 alloy showing Bi_2Te one-phase microstructure; (f) Bi80Te20 alloy showing Bi_7Te_3+(Bi) microstructure

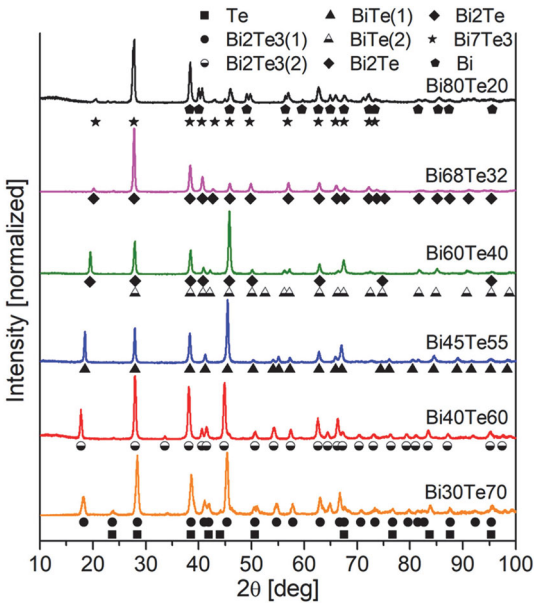

Fig. 4 X-ray powder diffraction pattern of annealed alloy samples no. 1-6: (a) no. 1-Bi30Te70, (b) no. 2-Bi40Te60, (c) no. 3-Bi45Te55, (d) no. 4-Bi60Te40, (e) no. 5-Bi63Te32, (f) no. 6–Bi80Te20. Bi_2Te_3(1) is represented by chart no. 01-076-2813, Bi_2Te_3(2) by chart no. 01-085-0439, BiTe(1) by chart no. 01-075-1095 and BiTe(2) is represented by chart no. 01-083-1749. (For representation of the references to colour in this figure legend, the reader is referred to the web version of this article)

stoichiometric parameters. Functions ${}^{0}G_{Bi}^{\mathrm{rom}}$ (GHSERBI) and ${}^{0}G_{Te}^{\mathrm{hex}}$ (GHSERTE) are Gibbs energies of pure Bi and Te in their SER reference state, respectively.

3.3.1 β(BiTe) Phase

β(BiTe) phase is treated as the phase with homogeneity range extending to Bi-rich side of compound. In order to describe the off-stoichiometric phase compositions, the anti-site atoms were introduced in the model. Therefore the $Bi_{0.4}(Bi, Te)_{0.6}$ model as in earlier assessments[12] and[13] was used to describe this homogeneity range. The Gibbs energy of this model (for one mole of atoms) has the following form:

$$ {}^{0}G_{Bi:Bi,Te}^{Bi_{0.4}Te_{0.6}} = y_{Bi}\,{}^{0}G_{Bi:Bi}^{Bi_{0.4}Te_{0.6}} + y_{Te}\,{}^{0}G_{Bi:Te}^{Bi_{0.4}Te_{0.6}} + 0.6\cdot RT(y_{Bi}\ln y_{Bi} + y_{Te}\ln y_{Te}) + y_{Bi}y_{Te}\sum_{i}{}^{i}L_{Bi:Bi,Te}^{Bi_{0.4}Te_{0.6}}(y_{Bi}-y_{Te})^{i} \quad \text{(Eq 3)} $$

where ${}^{0}G_{Bi:Bi}^{Bi_{0.4}Te_{0.6}}$ and ${}^{0}G_{Bi:Te}^{Bi_{0.4}Te_{0.6}}$ represent the Gibbs energies of Bi and $Bi_{0.4}Te_{0.6}$, respectively.

3.3.2 Bi_2Te_3 Phase

Gibbs free energy of binary stoichiometric Bi_2Te_3 compound is described by Wagner-Schottky defect model.[25] The model describes the composition range as a function of various defects. In this case the anti-site atoms defect describes very small homogeneity range of Bi_2Te_3 intermetallic compound as $(Bi,Te)_2(Bi,Te)_3$, which is in agreement with considerations by Xu et al.[39] and Hashibon and Elsässer.[40] Then Gibbs free energy is:

$$ {}^{0}G^{Bi_2Te_3} = y_{Bi}^{(1)}y_{Bi}^{(2)}\,{}^{0}G_{Bi:Bi}^{Bi_2Te_3} + y_{Te}^{(1)}y_{Te}^{(2)}\,{}^{0}G_{Te:Te}^{Bi_2Te_3} + y_{Bi}^{(1)}y_{Te}^{(2)}\,{}^{0}G_{Bi:Te}^{Bi_2Te_3} + y_{Te}^{(1)}y_{Bi}^{(2)}\,{}^{0}G_{Te:Bi}^{Bi_2Te_3} + {}^{id}G_{m}^{Bi_2Te_3} + {}^{ex}G_{m}^{Bi_2Te_3} \quad \text{(Eq 4)} $$

where ${}^{0}G_{i:j}^{Bi_2Te_3}$ (i, j = Bi, Te) is the Gibbs energy of end-member compounds when element i occupies sublattice (1), and element j occupies sublattice (2), y_i^s is fraction of element i in sublattice s (s = (1), (2))[41]. The Gibbs energy of ideal mixing is:

$$ {}^{id}G_{m}^{Bi_2Te_3} = RT\left[2\left(y_{Bi}^{(1)}\ln y_{Bi}^{(1)} + y_{Te}^{(1)}\ln y_{Te}^{(1)}\right) + 3\left(y_{Bi}^{2}\ln y_{Bi}^{(2)} + y_{Te}^{(2)}\ln y_{Te}^{(2)}\right)\right] \quad \text{(Eq 5)} $$

${}^{ex}G_{m}^{Bi_2Te_3}$ is the excess Gibbs energy of Bi_2Te_3 phase described by the parameters:

$$ L_{i:i,j}^{Bi_2Te_3} = L_{j:i,j}^{Bi_2Te_3} = L_{*:i,j}^{Bi_2Te_3} \quad \text{(Eq 6)} $$

$$ L_{i,j:i}^{Bi_2Te_3} = L_{i,j:j}^{Bi_2Te_3} = L_{i,j:*}^{Bi_2Te_3} \quad \text{(Eq 7)} $$

3.4 Liquid Phase

The liquid phase was described by an associate solution model,[23] which has been successfully previously adopted.[13] The liquid phase is assumed to have three species (i.e., Bi, Te and Bi_2Te_3). The Gibbs energy of the liquid is written as:

$$ {}^{0}G_{m}^{L} = y_{Bi}\,{}^{0}G_{Bi}^{L} + y_{Te}\,{}^{0}G_{Te}^{L} + y_{Bi_2Te_3}\,{}^{0}G_{Bi_2Te_3}^{L} + RT(y_{Bi}\ln y_{Bi} + y_{Te}\ln y_{Te} + y_{Bi_2Te_3}\ln y_{Bi_2Te_3}) + {}^{ex}G_{m}^{L} \quad \text{(Eq 8)} $$

where y_i is a molar fraction of species i (i = Bi, Te and Bi_2Te_3) in liquid phase, ${}^{0}G_{i}^{L}$ is a Gibbs energy of pure liquid species i. Excess Gibbs energy of liquid is denoted as ${}^{ex}G_{m}^{L}$, and T is an absolute temperature and R is a gas constant.

The expression of excess Gibbs energy of liquid has the form:

$$
\begin{aligned}
{}^{ex}G_m^L = {} & y_{Bi}y_{Bi_2Te_3}\sum_{i=0}^{n_1} {}^{i}L^L_{Bi,Bi_2Te_3}(y_{Bi}-y_{Bi_2Te_3})^i \\
& + y_{Bi_2Te_3}y_{Te}\sum_{i=0}^{n_2} {}^{i}L^L_{Bi_2Te_3,Te}(y_{Bi_2Te_3}-y_{Te})^i \qquad \text{(Eq 9)} \\
& + y_{Bi}y_{Te}\sum_{i=0}^{n_3} {}^{i}L^L_{Bi,Te}(y_{Bi}-y_{Te})^i
\end{aligned}
$$

where n_1, n_2, n_3 are respectively the degrees of the Redlich-Kister polynomial and parameters ${}^{i}L^L_{Bi(Te),Bi_2Te_3}$ are functions of temperature, in general like (1). To optimize this system the model parameters of liquid and Bi_2Te_3 phases were taken from Gierlotka[13] despite this description resulting in an inverted miscibility gap at T > 1587 °C. Considering the gas phase in thermodynamic calculations it is easy to show that this inverted miscibility gap occurs when the gas phase is the stable phase. Taking into account the available experimental information of this work together with reported data in literature the thermodynamic model parameters of Bi_7Te_3, Bi_2Te and BiTe were evaluated.

The results of the assessment obtained in the present work are presented in Tables 5 and 6. The phase diagram of Bi-Te system calculated from the present assessment is shown in Fig. 5.

4 Discussion

In the present discussion of the phase stability in Bi-Te system the data obtained for two ternary systems were also taken into consideration. Having in mind the future thermodynamic description of Ag-Bi-Te ternary system, the silver addition to Bi-Te phases is reviewed first.

Babanly et al.[28] reported the temperature evolution of EMF results obtained in several phase fields of Ag-Bi-Te system α′-Ag_2Te + Bi_2Te, α′-Ag_2Te + BiTe, and α′-Ag_2Te + BiTe + Bi_2Te_3. They used the electrochemical cell:

$$(-)\,Ag\,(solid)\,|\,Ag_4RbI_5(solid)\,|\,(Ag-Bi-Te)\,(solid)\,(+) \qquad \text{(Eq 10)}$$

for which as a solid electrolyte the solid superionic conductor Ag_4RbI_5 was used in relatively narrow temperature range 30–130 °C. The EMF measured in three-phase fields were reproduced upon repeated heating cycles of cells within the range of experimental errors. It means that the electrochemical cell (10) worked reversibly in the experimental temperature range which confirmed the stability of all three phases used as working electrode. Concluding, Babanly et al.[28] observed the existence of stable $Bi_{14}Te_6$ compound and Ag-, Bi_2Te-, BiTe-, and Bi_2Te_3-base solid solutions, which they denoted α, β, γ, and δ, respectively. The Bi_2Te_3-base solubility did not exceed 1 at.% Ag, which is consistent with Brebrick results.[24] The solubility of silver in the γ-BiTe and β-Bi_2Te phases was obtained up to ~ 2 at.% Ag at 230 °C. The boundaries between the solid solutions of intermediate phases in the Bi-Te system determined via EMF[28] agree with the data from physicochemical analysis.[29] It seems that these results have confirmed the stability of Bi_2Te and BiTe phases at low temperatures.

Very similar result was obtained by Prokhorenko et al.[31] using electrochemical cell:

$$(-)\,Ag\,|\,AgI\,|\,glass\,Ag_2GeS_3|K(+), \qquad \text{(Eq 11)}$$

where cell electrodes K are the equilibrated three-phase alloys in the Ag_2Te-Bi-Bi_2Te_3 region (Fig. 6), and (AgI | glass Ag_2GeS_3) is a two-layers membrane with Ag^+ ion conductivity. In such cell design the two-layers ion-selective membrane blocks the electron current in the electrochemical cell (11).[44] The temperature dependences of EMF values of cell (11) were studied in the range of 220–280 °C using the titration method.[45]

Also in this work, the obtained EMF results were reproduced upon repeated heating cycles of cells within the experimental error range. Such results confirm the stability of ternary phase fields in this system. Concluding, Prokhorenko et al.[31] noticed that Bi_2Te_3, BiTe, Bi_2Te, and $Bi_{14}Te_6$ phases of intermediate variable-composition form in the ternary Bi-Ag_2Te-Bi_2Te_3 system (Fig. 6). In their work,[31] the thermodynamic properties of saturated solid solutions of the $Bi_{14}Te_6$, Bi_2Te, BiTe, and Bi_2Te_3 phases in the Ag_2Te-Bi-Bi_2Te_3 system were determined using the EMF method.[33, 45, 46] The three-phase scheme of the ternary Ag_2Te-Bi-Bi_2Te_3 system within a temperature range of 300-600 K agrees well with the data of Babanly et al..[28, 32]

The existence of the compounds Bi_2Te_3, BiTe, Bi_2Te and $Bi_{14}Te_6$ has been also confirmed by Babanly's group[30] in the study of Bi-Te-I system. Besides the DTA and the XRD methods the thermodynamic properties in this system were also analysed by the measurements of electromotive forces of concentration cells with glycerine + KI saturated solution with small BiI_3 addition as the electrolyte. As a result of this study, the series of isopleths, isothermal section of the phase diagram at 300 K and a projection of the liquidus surface were constructed.[31]

In this work, Bi_2Te_3, BiTe and Bi_2Te compounds were synthesized by melting stoichiometric amounts of the corresponding pure, high grade elements under vacuum in quartz ampoules. Bismuth tellurides were synthesized by heating samples to ~ 900 K followed by slow cooling and annealing at temperatures below the corresponding peritectic reactions for 500–800 h. From the EMF

Table 5 The optimized parameters of the Bi-Te system

Parameters	Functions
Liquid	
${}^{0}G^{L}_{Bi_2Te_3}$	72794.5-22.082·T + 2·GLIQBI + 3·GLIQTE
${}^{0}L^{L}_{Bi,Bi_2Te_3}$	−159278.76 + 1.593·T
${}^{0}L^{L}_{Bi_2Te_3,Te}$	−258620.98 + 134.579·T
${}^{1}L^{L}_{Bi_2Te_3,Te}$	−140786.07 + 153.522·T
Bi_2Te_3	
${}^{0}G^{Bi_2Te_3}_{Bi:Bi}$	30000 + GHSERBI
${}^{0}G^{Bi_2Te_3}_{Te:Te}$	30000 + GHSERTE
${}^{0}G^{Bi_2Te_3}_{Bi:Te}$	−19087.09 + 3.74·T + 0.4·GHSERBI + 0.6·GHSERTE
${}^{0}G^{Bi_2Te_3}_{Te:Bi}$	0.0
${}^{0}L^{Bi_2Te_3}_{Bi,Te:Bi}$	10000-40.2·T
${}^{0}L^{Bi_2Te_3}_{Bi,Te:Te}$	10000-40.2·T
${}^{0}L^{Bi_2Te_3}_{Bi:Bi,Te}$	9800-41.0·T
${}^{0}L^{Bi_2Te_3}_{Te:Bi,Te}$	9800-41.0·T
Bi_2Te	
${}^{0}G^{Bi_2Te}_{Bi:Te}$	−35629.2-2.1144·T + 2·GHSERBI + GHSERTE
Bi_7Te_3	
${}^{0}G^{Bi_7Te_3}_{Bi:Te}$	−109514.1-3.729·T + 7·GHSERBI + 3·GHSERTE
β(BiTe)	
${}^{0}G^{\beta}_{Bi:Bi}$	+ 1474.3 + 9.747·T + GHSERBI
${}^{0}G^{\beta}_{Bi:Te}$	+ 232.47 + GBI2TE3
${}^{0}L^{\beta}_{Bi:Bi,Te}$	−6192.7-15.957·T
${}^{1}L^{\beta}_{Bi:Bi,Te}$	−877.59-5.5284·T
GBI2TE3	−19087.1 + 3.74·T + 0.4·GHSERBI + 0.6·GHSERTE

measurements the set of partial molar functions of bismuth in ternary alloys have been calculated as a function of temperature.[31]

It should be emphasized that in both analyses of ternary systems[28] and[31] the phase Bi_4Te_3 was not confirmed and the stable Bi_2Te compound was observed at room temperature.

In present work, the comparison of the results of the EDX and XRD analyses for as-cast alloys no. 3, 4 (with chemical composition Bi45Te55, Bi60Te40, respectively), Bi_2Te phase sample and annealed sample no. 4 (Bi60Te40 at.%) differ slightly, which may mean that one of the phases did not occur in a relevant volume in the alloys or that it was too little for the XRD equipment to detect. This confirms the unregular phase distribution in the as-cast alloys during fast cooling in cold water. Generally, the solidification of primary phases (Tab. 2) agrees with the solidification sequence according to the calculated phase diagram (Fig. 5).

Large grains of the primary phase Bi_2Te_3 and fine eutectic structure are visible in the sample of as-cast alloy no. 1 with the composition Bi30Te70 (Fig. 2a). The microstructure of the alloy with the Bi40Te60 composition studied by Zu et al.[47] looks very similar to as-cast alloy sample in this work. Whereas in this work, the microstructure of the as-cast sample no. 2 (Bi40Te60) practically does not contain the eutectic structure. It indicates a good agreement of the experimental alloy composition with the composition of the Bi_2Te_3 intermetallic compound.

The cooling rate has a significant impact on the degree of supercooling of the alloy, and on the phase crystallization sequence in a relevant alloys.[48, 49] The tendency to undercooling is greater when the solidification rate is increased. Huang et al.[48] investigated the peritectic reactions for the alloy with the atomic composition Bi60Te40. The cooling rate range was from 41.4 to $6{\cdot}10^5$ deg/min, which shows that the lower cooling value according to Huang et al.[48] was in fact quite high. Experimental results from the work[48] which indicate the crystallization of the metastable phases: Bi_4Te_5, Bi_4Te_3, is a consequence of

Table 6 The invariant reactions in the Bi-Te system calculated from present assessment

No.	Invariant reaction	Reaction temperature, °C	Liquid phase composition, x_{Te}	Reaction type	References
1	Liquid ↔ Bi_2Te_3	584.4	0.5997	Congruent melting	This work
		584.9	0.600		[10]
		589.0	0.600		[14]
		586.0	0.5995		[34]
		565.0	0.600		[51]
		586.0	0.600		[52]
2	Liquid + Bi_2Te_3 ↔ BiTe	559.5	0.456	Peritectic	This work
		561.6	0.477		[10]
		560.0	0.436		[12]
		540.0	0.440		[29]
		563.0	…		[34]
		562.0	0.500		[37]
		561.0	~ 0.500		[51]
3	Liquid + BiTe ↔ Bi_2Te	421.4	0.212	Peritectic	This work
		420.7	0.202		[10]
		420.0	0.205		[29]
4	Liquid ↔ Bi_2Te_3 + (Te)	415.6	0.886	Eutectic	This work
		413.1	0.908		[10]
		414.0	0.907		[12]
		413.0	0.900		[29]
		414.0	…		[37]
5	Liquid + Bi_2Te ↔ Bi_7Te_3	316.9	0.050	Peritectic	This work
		313.3	0.063		[10]
		312.0	0.055		[29]
		332.0	0.100		[52]
6	Liquid ↔ (Bi) + Bi_7Te_3	270.6	0.010	Eutectic	This work
		263.3	0.011		[10]
		266.0	0.024		[29]
		266.0	…		[37]
		264.0	0.025		[52]

strong tendency to undercooling the alloys in Bi-Te system.[49]

Glatz[37] studied alloys from the Bi-Te system and concluded that the eutectic on the bismuth side (266 °C) can be eliminated in the alloy with the atomic composition Bi56Te44 by equilibrating it at 300 °C for 180 days, while the equilibration at 250 °C for 90 days does not eliminate the eutectic reaction. For samples with a Te content greater than 40 at.%, which were equilibrated at 400 °C for 39 days, and at 300 °C for 180 days, the traces of Bi eutectic were still observed.[37] The data from Glatz's work[37] are consistent with the results obtained for the annealed alloy Bi60Te40 (Table 4, Fig. 4) in the present work – the eutectic is still present in this sample.

The (Bi) and Bi_8Te_3, (Bi) and Bi_8Te_3, Bi_8Te_3 phases were obtained in three equilibrated alloys with compositions Bi90Te10, Bi80Te20, Bi73Te27, respectively, by annealing them at 220 °C for 150 days during the studies carried out by Kifune et al.[26] The Bi_8Te_3 phase probably corresponds to the Bi_7Te_3 phase, which appears in the few studies as one of the intermetallic phases in Bi-Te system.[6, 7, 10] However, this probably indicates that there is also a certain range of non-stoichiometry of this phase, which has not been included in the representation of the Bi-Te phase diagram prepared by Chizhevskaya et al.[10] Additionally, the results of the sample with the composition Bi80Te20[26] are consistent with the results of the present work: at this chemical composition of the Bi-Te binary system the two-phase alloy was detected.

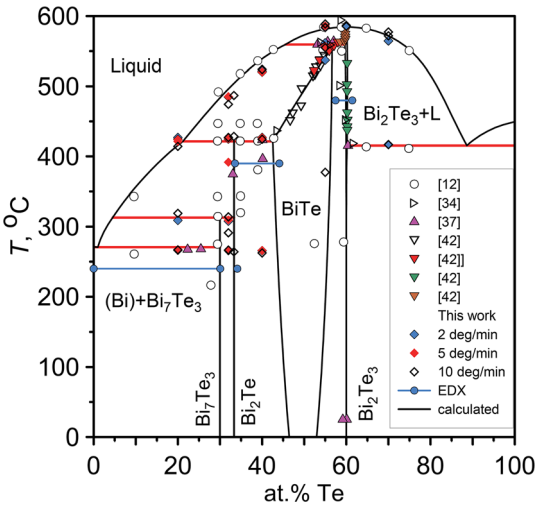

Fig. 5 Bi-Te phase diagram calculated from present assessment. The phase BiTe is modelled as β phase in [12] and [13]. Tie-lines are blue.

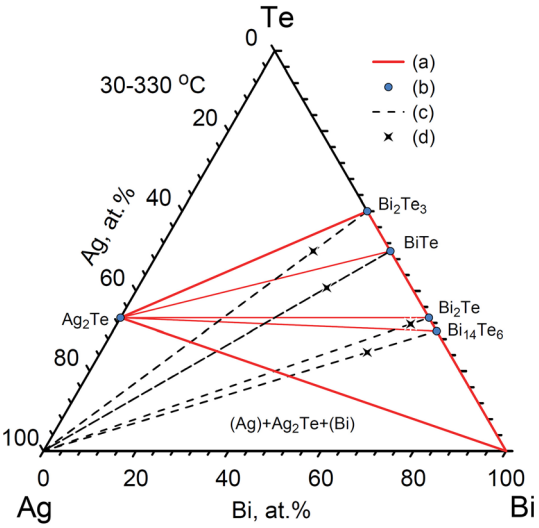

Fig. 6 The 3-phase fields of ternary Ag_2Te-Bi-Bi_2Te_3 system proposed by Prokhorenko et al.[31]. (a) pseudo-binaries between compounds (b), (c) the isopleths (Ag)–bismuth telluride. (d) Sample alloy compositions of the 3-phases electrode *K* of the experimental cells were superimposed[31].

X-ray powder diffraction pattern of annealed alloy samples no. 1–6 shown in Figure 4 present quite similar patterns to each other. This is due to the fact that the Bi_7Te_3, Bi_2Te, BiTe, Bi_2Te_3 phases are composed of the same structural units in different configurations of the atom layers: Te(1)Bi(1)Te(2)Bi(1)Te(1) (this layer cluster is only in Bi_2Te_3) and Bi(2)Bi(2).[6, 12, 27, 49–52]

Invariant reactions between the equilibrium phases are easier to observe during DTA analysis with low heating rates, e.g. 2 and 5 deg/min, which were also applied in the present work. The experimental DTA results are shown as diamond symbols in the proposed variant of the Bi-Te binary system (Fig. 5). Additionally, the DTA results were compared with the data of other researchers: Mao et al.[12] Brebrick,[24] Glatz,[37] Strassburger.[42] The experimental data of the present work do not coincide with the Bi-Te system proposed by Mao et al.[12] The Bi_4Te_3 phase does not occur in the equilibrated samples in present work (Table 4), and it was not recorded in the DTA measurements. The compound Bi_4Te_3, as well as Bi_4Te_5, Bi_6Te_7, Bi_8Te_9 phases are considered to be the metastable phases.[8, 27]

In addition, the samples of alloys (a–d) in Mao et al. work (Table 1 in[12]) were annealed for 30 days, which seems to be an insufficient period of time to reach the equilibrium in Bi-Te alloys.[37] It is also unlikely that the proposed β solution will exist in the Bi-Te binary system, as covalent-ionic interactions in intermetallic compounds do not allow for the formation of a structure with such a wide homogeneity range. Similar conclusions were obtained in the work of Stasova.[50] Basing on the XRD studies,[50] the presence of two intermetallic compounds in the binary system, Bi_2Te and BiTe, was confirmed. The BiTe phase was already obtained from very slow cooling, while the Bi_2Te phase required homogenizing equilibration. That observation was also confirmed by the results obtained in present study, where the following phases occurred in the unequilibrated sample of the Bi_2Te composition: BiTe and (Bi) (Table 2, Fig. 2g).

The present experimental DTA data and the similar data of Brebrick,[34] Glatz[37] and Strassburger[42] show very good agreement with the liquidus of the Bi-Te system developed by Chizhevskaya et al.[10] The only doubts are the points in the temperature range 260–390 °C for alloy no. 4 with the composition Bi60Te40. It is possible that the solubility of Bi in β(BiTe) phase is probably higher. To solve this problem some additional analyses are requested. On the other hand, the results for alloy no. 4 with the composition Bi60Te40 annealed at 265 °C confirm the presence of the Bi eutectic as in Glatz's work.[37] Therefore, for the alloys with similar compositions, it is necessary to equilibrate the samples over a 6 months period or longer.

After completion of the present work the latest topological data of Bi-Te system were published.[43] Hasanova et al.[43] proposed the new version phase diagram of Bi-Te system based on the study of long-term annealed samples of the bismuth-rich part of diagram studied by DTA, XRD, and SEM methods. To ensure homogeneous distribution of the elements in the samples, they were quenched from liquid state (430 °C) after alloying by dropping ampoules into water + ice mixture. Depending on the tellurium content the alloys were annealed at different temperatures for 43 days and then all samples were kept at 100 °C for 1 day. For comparison, they[43] synthesized several alloys of selected compositions by the traditional fusion method and annealed them under similar conditions.

Additionally, to the above used methods, the EMF study of concentration cell relative to Bi electrode with morpholine formate as an electrolyte was also performed. In the refined version of the phase diagram seven intermetallic compounds, Bi_2Te_3, Bi_4Te_5, Bi_8Te_9, BiTe, Bi_4Te_3, Bi_2Te, and Bi_7Te_3, with practically stoichiometric compositions were reported. All compounds, except Bi_2Te_3, melt incongruently in peritectic reactions. The EMF results were used to determine the partial molar thermodynamic functions of Bi in the alloys. Unfortunately, no BEI micrographs of annealed samples and no heating/cooling rate of DTA analysis were published. Anyhow, the results of experiments of Hasanova et al.[43] confirm that the Bi-Te system description with β-phase[12] and[13] seems to be wrong.

5 Conclusions

At the end, the following conclusions can be drawn:

- Scanning electron microscopy (SEM), X-ray diffraction (XRD) and differential thermal analysis (DTA) methods used to analyse the as-cast and equilibrated alloys of Bi-Te binary system confirmed the presence of the four intermetallic phases: Bi_2Te_3, β(BiTe), Bi_2Te and Bi_7Te_3. The presence of these phases suggests that the phase relations proposed in the descriptions of the binary system by Mao et al.[12] and Gierlotka[13] differ from the present study. Also, the primary solidified phases were identified from as-cast samples (Table 2).
- The model parameters of phases in Bi-Te system were assessed by optimization of available data by Calphad method. The thermodynamic assessments of Bi-Te system were compared taking also into account the latest experimental data of Hasanova et al.[43] The new optimized model parameters of Bi-Te system can form the basis for the design of thermoelectric materials based on bismuth and tellurium, especially with silver addition.
- The stability of intermetallic Bi_nTe_m phases in ternary systems was discussed. The phase sequence of Bi_2Te_3, β(BiTe), Bi_2Te, and Bi_7Te_3 ($Bi_{14}Te_6$) compounds in Bi-Te system is mentioned.

Acknowledgment This work was supported by the National Centre of Research and Development [Project Number: DKO/PL-TW1/5/2013 entitled: "Phase diagram determinations of thermoelectric materials"].

References

1. H.J. Goldsmid, and R.W. Douglas, The use of Semiconductors in Thermoelectric Refrigeration, *Br. J. Appl. Phys.*, 1954, **5**(11), p 386–390.
2. H. Goldsmid, Bismuth Telluride and its Alloys as Materials for Thermoelectric Generation, *Materials (Basel)*, 2014, **7**(4), p 2577–2592.
3. I.T. Witting, T.C. Chasapis, F. Ricci, M. Peters, N.A. Heinz, G. Hautier, and G.J. Snyder, The Thermoelectric Properties of Bismuth Telluride, *Adv. Electron. Mater.*, 2019, **5**(6), p 1–20.
4. R.F. Brebrick, *The Chemistry of Extended Defects in Nonmetallic Solids*, 1st edn. American Elsevier Publishing Company, Amsterdam, North-Holland, 1970.
5. J.S. Anderson, On Infinitely Adaptive Structures, *J. Chem. Soc. Dalt. Trans.*, 1973, **10**, p 1107.
6. J.W.G. Bos, H.W. Zandbergen, M.-H. Lee, N.P. Ong, and R.J. Cava, Structures and Thermoelectric Properties of the Infinitely Adaptive Series $(Bi_2)_m(Bi_2Te_3)_n$, *Phys. Rev. B*, 2007, **75**(19), p 195203.
7. H. Okamoto and L. E. Tanner, Bi-Te (Bismuth-Tellurium) Binary Alloy Phase Diagrams, in *Binary Alloy Phase Diagrams*, 2nd ed., T. B. Massalski and H. Okamoto, Eds. Ohio, USA: Materials Park, ASM International, 1990, pp. 800–801
8. F. Hulliger, Structural Chemistry of Layer-Type Phases, *Physics and Chemistry of Materials*, vol. 5., F. Lévy, Ed. Dordrecht, Holland/ Boston, USA: D. Reidel Publishing Company, 1976
9. S. Chen, S. Lu, and J. Chang, Bi-In-Te Phase Diagram, *J. Alloys Compd.*, 2017, **722**, p 499–508.
10. S.N. Chizhevskaya, L.E. Shelimova, W.S. Zemskov, W.I. Kosyakov, and D.W. Malakov, Critical Assessment and Fitting of Data on the Bi-Te Phase Diagram, *Neorg. Mater.*, 1994, **30**(1), p 3–11. **in Russian**
11. G.A. Malahov, S. W. Zvykin, and W. I. Kosjakov (1989) Elektricheskie Svoistva Splavov Wizmuta I Osnovy Metoda. *Zhurnal Fiz. Khimii (Russian J. Phys. Chem.)* 63(2): 328-333
12. C. Mao, M. Tan, L. Zhang, D. Wu, W. Bai, and L. Liu, Experimental Reinvestigation and Thermodynamic Description of Bi-Te Binary System, *Calphad*, 2018, **60**, p 81–89.
13. W. Gierlotka, A New Thermodynamic Description of the Binary Bi-Te System Using the Associate Solution and the Wagner-Schottky Models, *Calphad*, 2018, **63**, p 6–11.
14. B.W. Howlett, S. Misra, and M.B. Bever, On the Thermodynamic Properties of the Compounds Sb_2Se_3, Bi_2Se_3, Sb_2Te_3 and Bi_2Te_3, *Trans. Metall. Soc. AIME*, 1964, **230**(10), p 1367–1372.
15 Z. Boncheva-Mladenova, A.S. Pashinkin, and A.V. Novoselova, Investigation of the evaporation of antimony and bismuth tellurides and of bismuth selenide, in *Chemical Bonds in Solids*. N.N. Sirota, Ed., Springer US, Boston, MA, 1995, p151–158. https://doi.org/10.1007/978-1-4684-1686-2_26
16. A.A. Vecher, L.A. Mechkovskii, and A.S. Skoropanov, Determination of the Heat of Formation of Certain Tellurides, *Izv.*

Akad. Nauk SSSR Neorg. Mater. (Inorganic Mater.), 1974, **10**, p 2140–2143.
17. D.D. Wagman, W.H. Evans, V.B. Parker, R.H. Schumm, I. Halow, S.M. Bailey, K.L. Churney, and R.L. Nuttall, The NBS Tables of Chemical Thermodynamic Properties, *J. Phys. Chem. Ref. Data.*, 1982, **11**, Suppl. 2, p 2-81.
18. V.R. Sidorko, L.V. Goncharuk, and R.V. Antonenko, Thermodynamic Properties of Bismuth Sesquiselenide and Sesquitelluride and Their Solid Solutions, *Powder Metall. Met. Ceram.*, 2008, **47**(3–4), p 234–241.
19. R. Castanet, and M. Laffitte, Enthalpie de Formation, Diagramme de phases et Structure du Système Ternaire Tellure-Bismuth-Antimoine à 737 K (Enthalpy of Formation, Phase Diagram and Structure of the Tellurium-Bismuth-Antimony Ternary System at 737 K), *J. Less Common Met.*, 1975, **40**(2), p 221–234. **in French**
20. V.M. Glazov, L.M. Pavlova, and Y.V. Yatmanov, A Thermodynamic Assessment and Experimental Verification of the Possibility of Diffusionless Crystallisation of Alloys in the Bi-Te System, *Russ. J. Phys. Chem.*, 1984, **58**, p 176–180.
21. Y. Tachikawa, Y. Tsuchiya, F. Kakinuma, and T. Itami, Sound Velocity in the Molten Bi-Te Alloy, *J. Non. Cryst. Solids*, 2016, **435**, p 48–54.
22. F.A. Kanda, and R.P. Colburn, The Absolute Viscosity of Some Bismuth-Tellurium Alloys, *High Temp. Sci.*, 1973, **5**(3), p 83–88.
23. F. Sommer, Association Model for Description of the Thermodynamic Functions of Liquid Alloys, *Zeitschrift fuer Met. Res. Adv. Tech.*, 1982, **73**(2), p 72–76.
24. R.F. Brebrick, Homogeneity Ranges and Te_2-Pressure Along the Three-Phase Curves for Bi_2Te_3(c) and a 55–58 at.% Te, Peritectic Phase, *J. Phys. Chem. Solids*, 1969, **30**(3), p 719–731. https://doi.org/10.1016/0022-3697(69)90026-2
25. F. Zhang, W. Huang, and Y.A. Chang, Equivalence of the Generalized Bond-Energy Model, the Wagner-Schottky-Type Model and the Compound-Energy Model for Ordered Phases, *Calphad*, 1997, **21**(3), p 337–348.
26. K. Kifune, T. Tachizawa, H. Kanaya, Y. Kubota, N. Yamada, and T. Matsunaga, Boundaries of the Homologous Phases in Sb-Te and Bi-Te Binary Alloy Systems, *J. Alloys Compd.*, 2015, **645**, p 382–387.
27. L.E. Shelimova, O.G. Karpinskii, V.I. Kosyakov, V.A. Shestakov, V.S. Zemskov, and F.A. Kuznetsov, Homologous Series of Layered Tetradymite-Like Compounds in Bi-Te and GeTe-Bi_2Te_3 Systems, *J. Struct. Chem.*, 2000, **41**(1), p 81–87.
28. M.B. Babanly, Y.M. Shykhyev, N.B. Babanly, and Y.A. Yusibov, Phase Equilibria in the Ag-Bi-Te System, *Russ. J. Inorg. Chem.*, 2007, **52**(3), p 434–440.
29. N.K. Abrikosov, V.F. Bankina, L.V. Poretskaya, L.E. Shelimova, and E.V. Skudnova, *Semiconducting II-VI, IV-VI, and V-VI Compounds*. Springer Science + Business Media, LLC, Moscow, 1969.
30. M.B. Babanly, J.C. Tedenac, Z.S. Aliyev, and D.V. Balitsky, Phase Equilibriums and Thermodynamic Properties of the System Bi-Te-I, *J. Alloys Compd.*, 2009, **481**(1–2), p 349–353.
31. M.V. Prokhorenko, M.V. Moroz, and P.Y. Demchenko, Measuring the Thermodynamic Properties of Saturated Solid Solutions in the Ag_2Te-Bi-Bi_2Te_3 System by the Electromotive Force Method, *Russ. J. Phys. Chem. A*, 2015, **89**(8), p 1330–1334.
32. M. Babanly, Y. Yusibov, and N. Babanly, The EMF Method with Solid-State Electrolyte in the Thermodynamic Investigation of Ternary Copper and Silver Chalcogenides, *Electrom. Force Measurem. Sev. Syst. InTech*, 2011, **21**, p 57–78.
33. A. G. Morachevskii, G. F. Voronin, V. A. Geiderikh, and I. B. Kutsenok, *Electrochemical Research Methods in Thermodynamics of Metallic Systems*, Moscow, Russia: Akademkniga, 2003.
34. R.F. Brebrick, Tellurium Vapor Pressure and Optical Density at 370–615 °C, *J. Phys. Chem.*, 1968, **72**(3), p 1032–1036.
35. R.F. Brebrick, and F.T.J. Smith, Partial and Total Vapor Pressures Over Molten Bi_2Te_3, *J. Electrochem. Soc.*, 1971, **118**(6), p 991.
36 R. Viswanathan, R. Balasubramanian, D. Albert Raj, M. SaiBaba, and T.S.L. Narasimhan, Vaporization Studies on Elemental Tellurium and Selenium by Knudsen Effusion Mass Spectrometry, *J. Alloys Compd.*, 2014, **603**, p 75–85.
37. A.C. Glatz, An Evaluation of the Bismuth-Tellurium Phase System, *J. Electrochem. Soc.*, 1965, **112**(12), p 1204–1207.
38. Scientific Group Thermodata Europe, Unary Database v. 5.0, 2009, Available: https://www.sgte.net/en/free-pure-substance-database
39 Z. Xu, H. Wu, T. Zhu, C. Fu, X. Liu, L. Hu, J. He, J. He, and X. Zhao, Attaining High Mid-Temperature Performance in (Bi, Sb)2Te3 Thermoelectric Materials Via Synergistic Optimization, *NPG Asia Mater.*, 2016, **8**, p 1–9.
40. A. Hashibon, and C. Elsässer, First-Principles Density Functional Theory Study of Native Point Defects in Bi_2Te_3, *Phys. Rev. B*, 2011, **84**, p 144117.
41. H. Lukas, S.G. Fries, and B. Sundman, *Computational Thermodynamics*. Cambridge University Press, Cambridge, 2007.
42. J. Strassburger, Phase Studies Using the Traveling Solvent Method of Crystal Growth: The Bismuth-Tellurium System, *J. Electrochem. Soc.*, 1969, **116**(5), p 640–645.
43. G.S. Hasanova, A.I. Aghazade, S.Z. Imamaliyeva, Y.A. Yusibov, and M.B. Babanly, Refinement of the Phase Diagram of the Bi-Te System and the Thermodynamic Properties of Lower Bismuth Tellurides, *JOM*, 2021, **73**(5), p 1511–1521.
44. M.V. Moroz, M.V. Prokhorenko, and P.Y. Demchenko, Thermodynamic Properties of the Intermediate Phases of a Ag-Te-AgBr System, *Russ. J. Phys. Chem. A*, 2013, **87**(1), p 6–9.
45. M.V. Voronin, and E.G. Osadchii, Standard Thermodynamic Properties of Ag_3Sb and Ag_6Sb Evaluated by EMF Measurements, *Inorg. Mater.*, 2013, **49**(6), p 550–554.
46. M. B. Babanly, Y. A. Yusibov, and V. T. Abishov (1992) The Method of Electromotive Forces in the Thermodynamics of Complex Semiconductor Materials. *Monogr. Baku*: Russian p 323
47. F.Q. Zu, Z.Y. Huang, Z.Z. Wang, X. Cui, and X.Y. Li, Abnormal Solidification of BiTe Alloys Induced by Liquid Structural States, *Mater. Sci. Semicond. Process.*, 2010, **13**(2), p 86–91.
48. Z. Huang, F. Zu, J. Chen, and G. Ding, The Dependence of Phase Selection in Peritectic Solidification of Bi-Te40 on Cooling Rates and Liquid States, *Intermetallics*, 2010, **18**(5), p 749–755.
49. J.H. Perepezko, Nucleation Reactions in Undercooled Liquids, *Mater. Sci. Eng. A*, 1984, **65**(1–2), p 125–135.
50. M.M. Stasova, X-ray investigation of some bismuth and antimony chalcogenides, *J. Struct. Chem.*, 1965, **5**(5), p 731–732.
51. T. Shimazaki, and H. Ozawa, Tsumonite, BiTe, a new mineral from the Tsumo mine Japan, *Am. Mineral.*, 1978, **63**, p 1162–1165.
52. K. Yamana, K. Kihara, and T. Matsumoto, Bismuth Tellurides: BiTe and Bi_4Te_3, *Acta Crystallogr. Sect. B Struct. Crystallogr. Cryst. Chem.*, 1979, **35**(1), p 147–149.